Modulating Microglial Activation using MAPK and Arginase Inhibitors in Alzheimer's Diseased Mouse Models

Benjamin Ahn
BIOL Research 4699
21 April 2020

ABSTRACT

Microglia are brain resident macrophages and serve as immune effector cells, maintaining homeostasis in the brain. Depending on their surrounding environment, microglia dynamically morph between two polarized states - pro-inflammatory and anti-inflammtory. These activation states are regulated by cytokine feedback loops in which previous studies have demonstrated the potential to control these pathways via inhibitors. Nx-hydroxynor-arginine (nor-NOHA) inhibits arginase, an enzyme that plays a role in promoting the anti-inflammatory pathway. SB-203580 (SB) inhibits p38 in the MAPK pathway that promotes a pro-inflammatory pathway. In a healthy central nervous system, these microglial dynamics are maintined in homeostasis, however in Alzheimer's Disease (AD), microglia are chronically activated, resulting in neuroinflammation and disease pathology.

This experiment investigates the effects of nor-NOHA and SB on microglial activation and whether inhibitors can be used to correct microglial activation in Alzheimer's Disease using *in vivo* mouse models. 5xFAD mice were administered a series of intraperitoneal injections of control, lipopolysaccharide (LPS), nor-NOHA, and/or SB. The mice were anesthetized, and their brains were analyzed via immunohistochemistry, staining for Iba-1, a common pro-inflammatory marker. Microglial activation was quantified by measuring Iba-1 expression and microglial morphology.

When quantifying Iba-1 expression, the results were inconclusive, with nor-NOHA showing no clear effect on microglial activation. When quantifying microglial morphology such as branch length and ramification, experimental groups treated with nor-NOHA displayed an increase in pro-inflammatory microglia, and those treated with nor-NOHA and then SB displayed a decrease in pro-inflammatory microglia.

The results show limited promise of nor-NOHA and SB acting as effective inhibitors, however a more thorough image analysis must be conducted. 3D computational methods should be used to further analyze the microglial morphology from this experiment. If microglial activation can be controlled via inhibitors, this may lead to novel therapeutic strategies that involve correcting chronically activated microglia in AD. If such promise is shown, additional *in vivo* testing should be done to analyze the effects of modulated microglial activation on neurons. The ability to control and modulate microglial activation using inhibitors may lead to novel therapeutics that enable the rescue and recovery of disease physiology of microglia for several neurodegenerative diseases.

INTRODUCTION

Microglia are the brain-resident immune cells responsible for maintaining brain homeostasis, immune response, development, and repair. In response to injury or infection, microglia become pro-inflammatory, exhibiting increased expression of pro-inflammatory cytokines and ionized calcium binding adapter molecule 1 (Iba1-1) (Cherry *et al.*). Pro-inflammatory microglia resemble a highly ramified morphology with stretched out processes whereas anti-inflammatory microglia resemble an amoeboidic morphology with limited primary branches (Fernandez-Arjona *et al.*). Pro-inflammatory microglia play a role in removing debris through phagocytosis. When aiding in tissue repair, microglia become anti-inflammatory and exhibit increased

expression of arginase (Sarlus and Heneka). These two activation states represent two extremes of a gradient of activation states that microglia can demonstrate and transition between.

A network of intra-cellular signaling pathways regulate microglial activation such as Mitogen-activated protein kinase (MAPK) pathways (Kaminska *et al.*). MAPK is a collection of protein kinase cascades including p38 (Herlaar and Brown), which are activated by pro-inflammatory mediators such as LPS and TNFalpha and upregulate pro-inflammatory microglia (Morrison). To upregulate anti-inflammatory state, arginase-1, an enzyme responsible for (Cherry *et al.*). Previous research has shown that cytokine and enzyme inhibitors can change microglia physiology. nor-NOHA, an arginase inhibitor, has been shown to effectively reduce microglia arginase activity (Lisi *et al.)*. SB is a p38 inhibitor which has been shown to block the MAPK pathway and reduce inflammation (Kankaanranta *et al.*).

In a healthy immune system, microglial pro-/anti-inflammatory activation states are regulated and in homeostasis. In AD, microglia become chronically pro-inflammatory. The accumulation of amyloid beta results in the pro-inflammatory activation of microglia, which through cytokine feedback loops, results in further microglia activation and a cycle that results in neuroinflammation (Cherry *et al.*). Although they play a role in amyloid beta clearance, unregulated pro-inflammatory microglia result in tissue damage, neurotoxicity, and associated disease pathology.

Previous research in this field has primarily focused on the induction of anti-inflammatory conditions to assuage disease pathology, but this approach has shown limited success. Minimal research has been conducted on restoring microglial function by manipulating their inflammatory states. A model that can correct microglial activation such that it mirrors healthy microglia physiology might provide more beneficial outcomes in an AD environment. This experiment aims to use nor-NOHA, an arginase inhibitor, and SB, a p33 MAPK inhibitor, to manipulate microglial activation in 5xFAD mouse models. Microglial activation was characterized using immunofluorescence and morphology analysis.

METHODS

Experimental Treatments

Male and female, wild-type and 5xFAD mice were carried out to ten weeks of age. For each gender and disease phenotype combination, they were split into four experimental groups, consisting of a series of intraperitoneal injections of vehicle control, 4xLPS, 4x LPS with nor-NOHA, or 4x LPS with nor-NOHA then SB. Experimental groups with multiple IP injections were administered in 24 hour increments.

Figure 1. *Experimental setup showing conditions.* Mice were split into four groups according to gender and disease phenotype. For each group, a mouse was administered one of four IP injection treatments with 24 hour wait periods between injections if applicable. The figure displays the treatment setup for one gender/disease phenotype group however the same set-up was used for all four gender/disease phenotype groups.

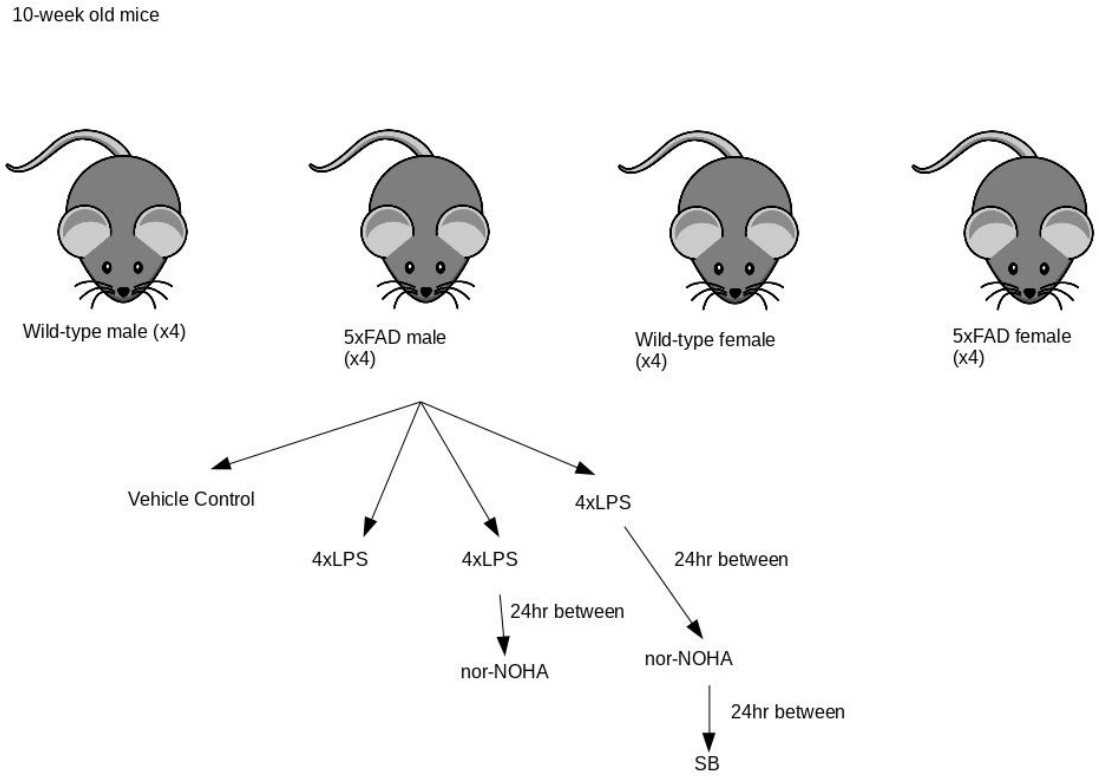

Tissue Preparation and Immunofluorescent Staining

The mice were anesthetized using isoflurane, and put down via cervical dislocation. The brains were extracted from 10-week old mice and fixed in 4% PFA and then saturated in 30% sucrose for 48 hours until the brains were sunk a the bottom of a 15 mL tube. Brain samples were then prepared in Optimal Cutting Medium, and 40 um sagittal sections were cut using a cryostat which were collected in phosphate-buffered saline (PBS). Sections were rinsed three times with PBS and stored in 0.2% sodium azide.

Free-floating immunohistochemistry was performed in 24-well plates. Sections were blocked in LI-COR blocking buffer (LBB) and then rinsed three times in PBS. Sections were then stained with anti-Iba1 (1:500 in LBB, rabbit) and Alexa-fluor 555 (1:200 in LBB, anti-rabbit) antibodies. Slices were then washed twice in PBS. Nuclei were then stained with DAPI (1:1000 in PBS). Sections were mounted on microscope slides and covered with a coverslip using vectashield mounting medium. Each batch of histology did not have samples from all mouse animals. For each batch, one animal for each treatment type for one gender was used.

Imaging and Image Processing

Images were acquired using a Zen immunofluorescent microscope with 20x magnification in z-stacks with 1um-thick slices. Images of the CA3, CA2, and CA1 regions of the hippocampus as well as the cortex were taken. Images were acquired throughout the course of two days. Background and foreground levels were adjusted manually in Zen Blue for each z-stack and exported as TIF files.

Data Analysis of Iba1 Fluorescence and Microglia Morphology

All image and data analysis used self-developed custom scripts with the exception of plug-ins and analysis toolboxes.

Maximum Intensity Projections (MIP) were created from each z-stack in ImageJ.
Iba-1 expression was quantified using integrated fluorescent intensity normalized to cell count and time in MATLAB.

Average branch length was quantified first by processing MIPs to remove background, sharpen contrast, and binarize in ImageJ (Young and Morrison). The Skeleton (2D/3D) and AnalyzeSkeleton ImageJ plug-ins were then applied to each binarized image (Arganda-Carreras, *et al.*). Branch lengths were calculated and averaged for each MIP, excluding skeletons below a specified threshold length in R Studio (R Core Team). The average branch length for each image was plotted in MATLAB.

Skeletonized images from the average branch length quantification where then used to quantify ramification. A six-by-nine non-destructive grid was applied to each image, and a random number generator was used to randomly select five microglia per image. The Sholl Analysis ImageJ plug-in was used to calculate a Ramification Index (Stanko *et al*). The ramification data was then plotted in MATLAB.

All scripts are made available on https://github.com/1100266506/microglia_modulation_cytokineinhibitors.

Figure 2. *Image processing steps to measure average branch length and ramification index.*(A) Maximum Intensity Projections (MIP) were created for each z-stack image. (B) Channels were then split to isolate the channel representing Iba-1. (C) After auto-enhancing contrast, applying an unfiltered mask, and despeckling the image, the image was binarized. (D) The Skeletonize (2D/3D) plugin was used to create skeletonized branches and measure branch lengths. (E) A non-destructive grid was applied to allow for randomized selection of microglia. (F) Five microglia per image were randomly selected to conduct a Sholl Analysis. All image processing steps were conducted in ImageJ.

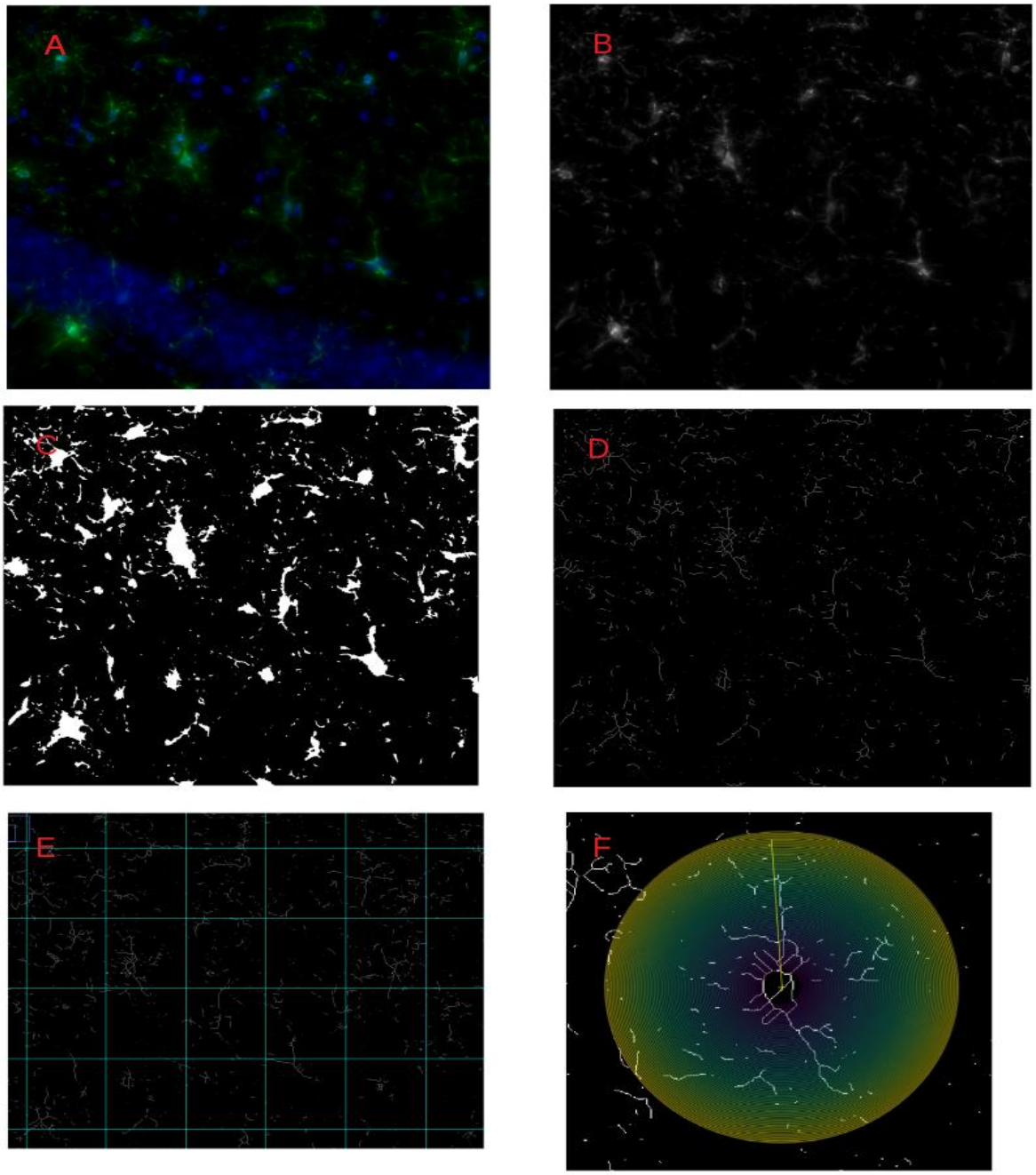

DATA AND RESULTS

Figure. 3. *Immunofluorescent Maximum Intensity Projections of male cortex regions stained for Iba-1 and DAPI.* Three images per histology sample were taken of the cortex region of the brain, and each experimental condition had a sample size of at least 3 or more. Iba-1 is stained to show microglial activation, morphology, and cell count.

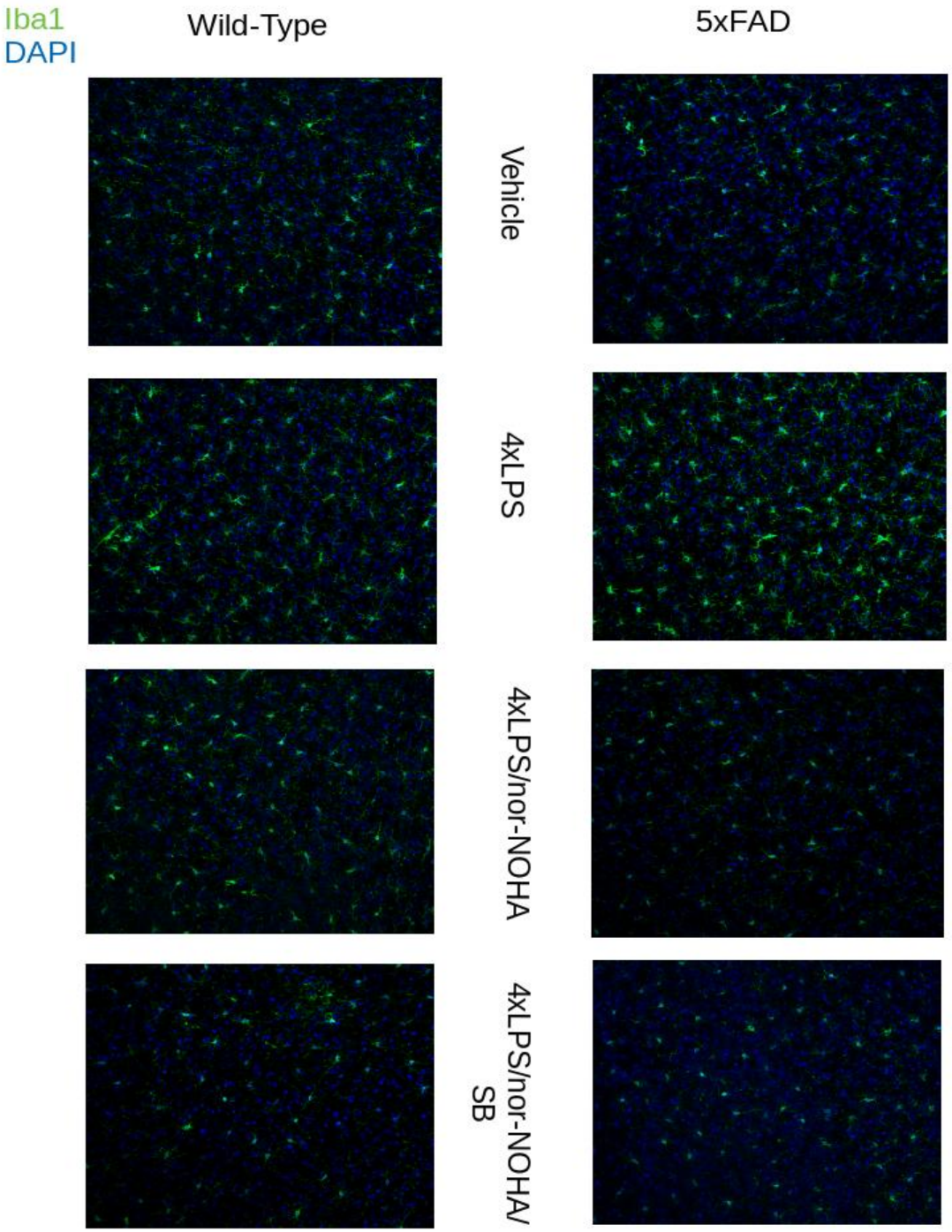

Figure 4. *Integrated immunofluorescence normalized to cell count of Iba-1 expression from microglia in the hippocampal and cortical regions.*

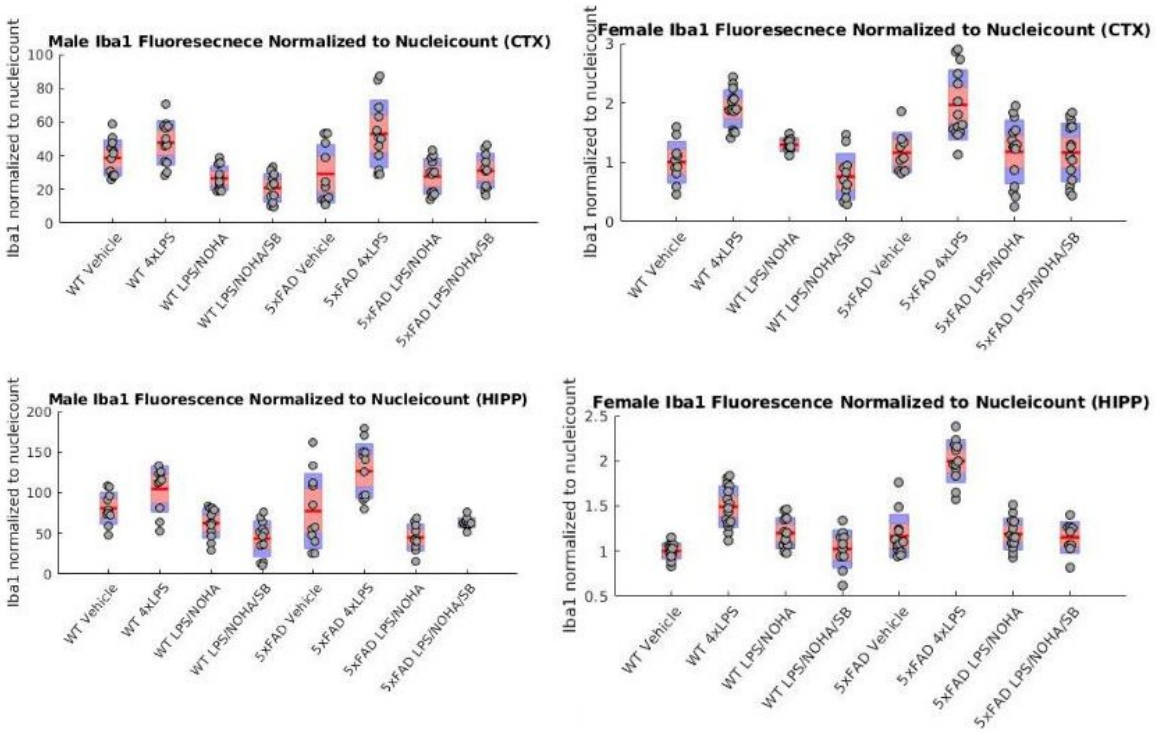

Figure 5. *Iba-1 positive microglia count normalized to cell count in hippocampal and cortical brain regions.*

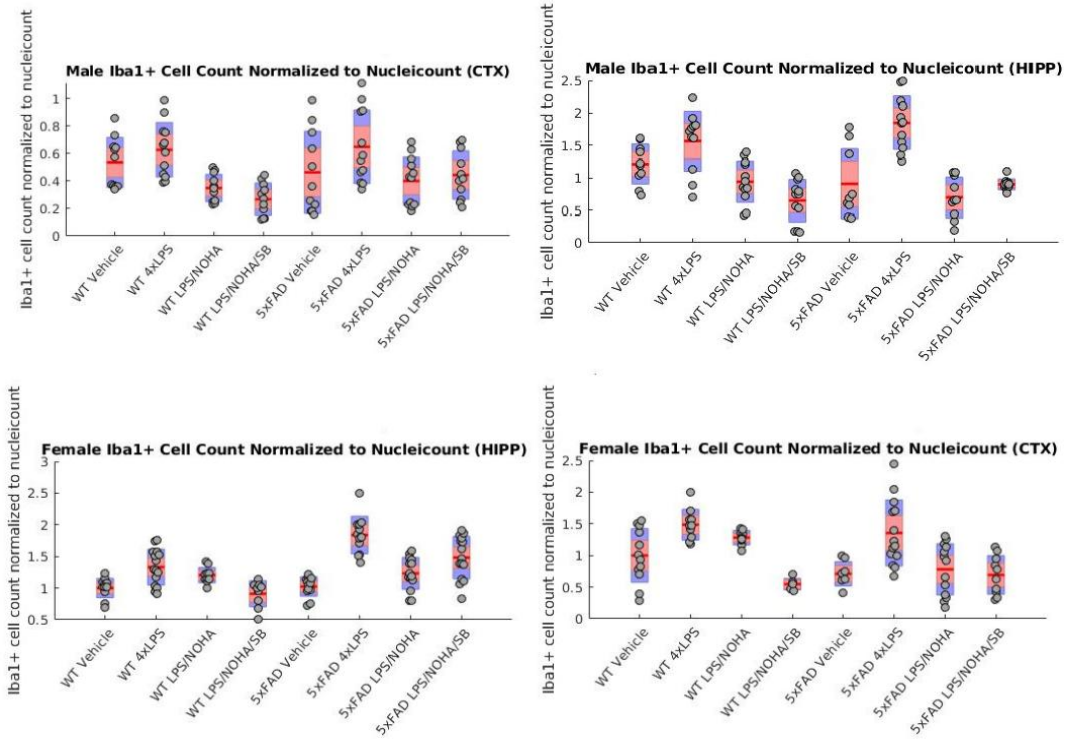

Figure 6. *Average branch length normalized to cell count in hippocampal and cortical brain regions.*

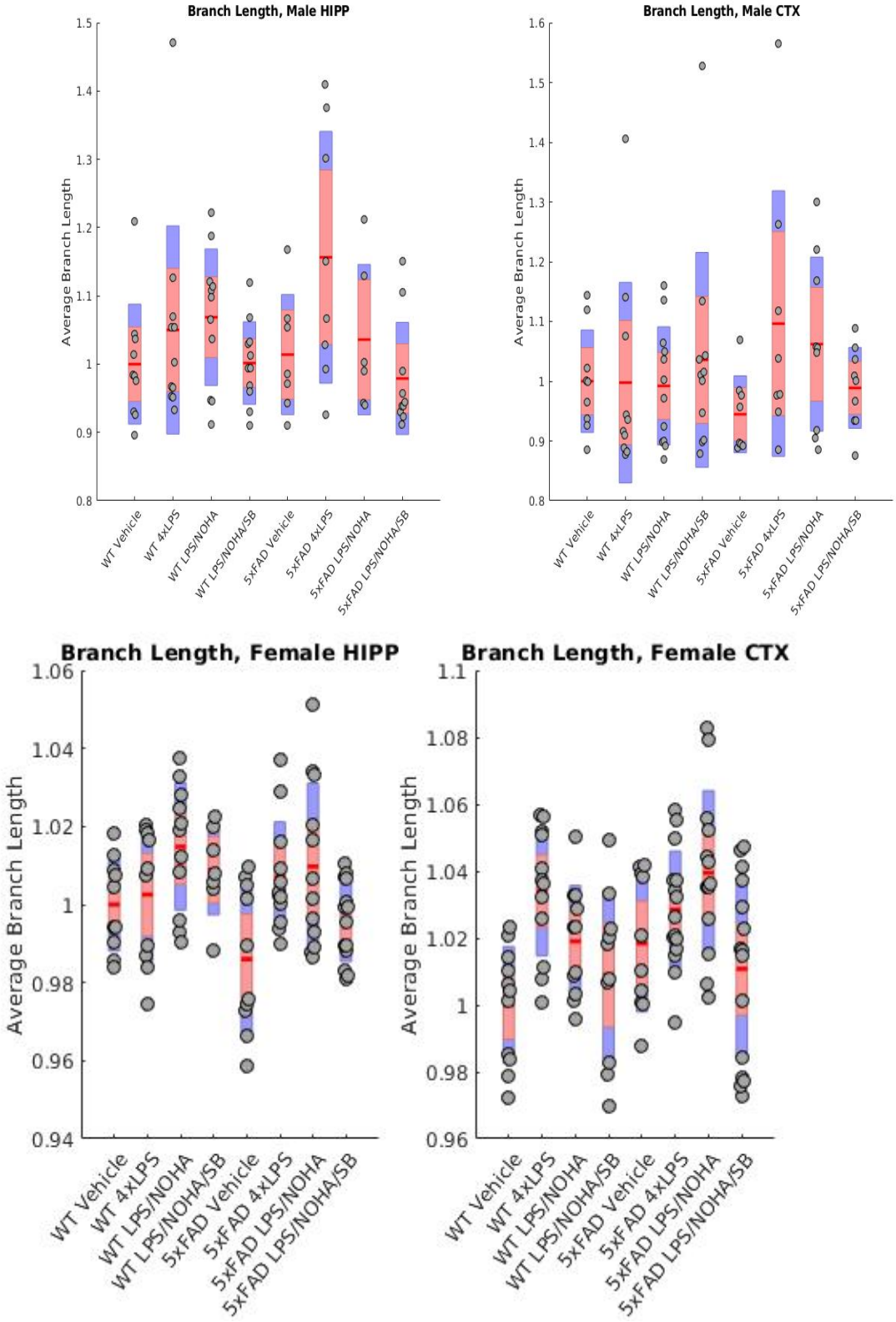

Figure 7. *Ramification Index from Sholl Analysis in hippocampal and cortical brain regions*. For the wild-type, at least 30 microglia were analyzed per group. For the 5xFAD, at least 15 microglia were analyzed per group.

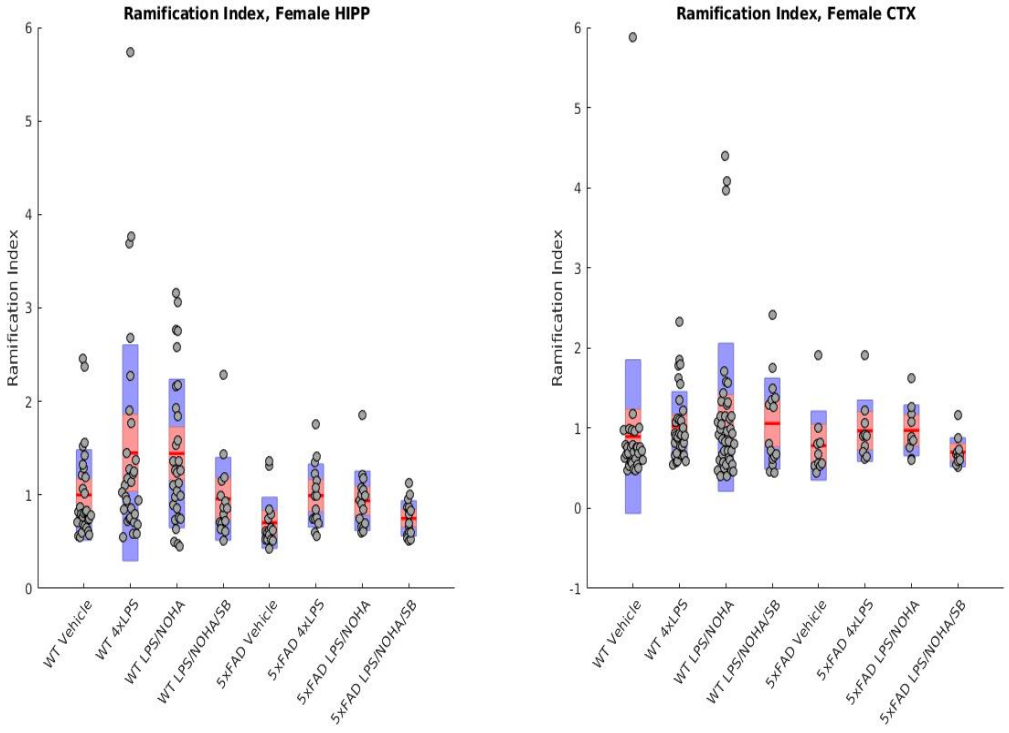

DISCUSSION

The data fail to show a clear impact from the nor-NOHA and SB inhibitors on pro-inflammatory microglial activation. nor-NOHA shows contradictory effects on microglial activation while SB shows a weak ability to decrease microglial activation.

Quantifying Microglial Activation via Iba-1 Expression

When quantifying microglial activation via Iba-1 immunofluorescence, nor-NOHA failed to increase while SB greatly decreased pro-inflammatory activation of microglia. Upon visual inspection, Iba-1 expression is greater in the 4xLPS groups than the vehicle groups for both male and female and wild-type and 5xFAD which verify our control groups (figure 3). Iba-1 immunofluorescence however decreased in the 4xLPS/nor-NOHA group in comparison to the 4xLPS group (figure 3), when we expected an increase. nor-NOHA acts as an inhibitor to the microglial anti-inflammatory pathway, which as a result, should increase pro-inflammatory microglial activation. When quantifying the immunofluorescence, the data matched the visual observations, mirroring a decrease in Iba-1 immunofluorescence for 4xLPS/nor-NOHA groups across both genders, phenotypes, and brain regions (figure 4).

Iba-1 immunofluorescence in the 4xLPS/nor-NOHA/SB group decreased in comparison to the 4xLPS groups (figure 3), however these results were expected. SB acts as an inhibitor to p38, which is a critical mediator for the MAP-K pathway that increases pro-inflammatory microglial activation. Thus, interference with p38 through SB would have decreased pro-inflammatory activation and levels of Iba-1 expression. The quantification displayed similar results to the

visual observations, showing a decrease in Iba-1 immunofluorescence across both genders, phenotypes, and brain regions (figure 4). Although we fail to see additional pro-inflammatory activation from the nor-NOHA, we have some evidence that SB can reduce pro-inflammatory activation after stimulation from 4xLPS.

The results showed similar trends when quantifying Iba-1 positive microglia. We fail to see gliosis and an increase in microglia cells, indicated by the decrease in number of Iba-1 positive microglia in the 4xLPS/nor-NOHA group compared to the 4xLPS groups (figure 5). However, we continue to see a strong decrease in pro-inflammatory activation, also shown by the decrease in number of Iba-1 positive microglia (figure 5). Although not significant, 4xLPS/nor-NOHA/SB groups showed a lower magnitude of microglial activation in both Iba-1 immunofluorescence and Iba-1 positive microglia cells compared to the 4xLPS/nor-NOHA groups in most experimental groups. This suggests that SB still might have a decreasing effect on microglial activation, but a different quantification method would be needed.

Quantifying Miroglial Activation via Morphology

When quantifying microglial morphology, nor-NOHA showed a weak increase in microglial activation, and SB showed a decrease in microglial activation. An average branch length and Ramification Index were used to quantify morphology, with a greater average branch length and higher ramification index indicating more pro-inflammatory microglia. Despite wide variation, the 4xLPS groups show a greater average branch length and ramification index in most experimental groups, which verifies our control groups.

The 4xLPS/nor-NOHA groups showed an increase in average branch length in comparison to the 4xLPS groups in the hippocampal regions for both genders but only the wild-type groups. The other experimental groups showed either the same or a slight decrease in average branch length for the 4xLPS/nor-NOHA groups in comparison to the 4xLPS groups (figure 6). The 4xLPS/nor-NOHA groups also show only a slight increase in ramification index in comparison to the 4xLPS groups (figure 7). This suggests that nor-NOHA may not have a strong effect on pro-inflammatory activation.

The 4xLPS/nor-NOHA/SB groups showed a modest decrease in average branch length and ramification index in comparison to the 4xLPS and 4xLPS/nor-NOHA groups (figure 6 and 7). The distribution of the 4xLPS/nor-NOHA/SB groups show a smaller variation compared to other groups which somewhat strengthen the data.

Because of some contradictory results and no significant difference between experimental groups, no meaningful conclusion can be made regarding the effect of nor-NOHA or SB on microglial activation. However, we do see a directional trend of the 4xLPS/nor-NOHA/SB groups decreasing microglial activation compared to the 4xLPS and 4xLPS/nor-NOHA groups in when analyzing both Iba-1 expression levels and microglia morphology. **This suggests that SB might still act as a pro-inflammatory reducing mediator.**

Although our morphology data has been validated by previous studies, additional morphology studies should be conducted. This experiment used 2D computational methods while new, more effective 3D computational methods have been developed (Heindi *et al.*). Microglia are complex, 3D cells in which morphological data can be lost when analyzing only 2D images. 3D analysis can capture a more accurate measure of microglia morphology while reducing user bias by using computational rather than manual methods.

Use of inhibitors as means to control microglial activation still remain to be explored. These results showed some promise, particularly with SB and its ability to reverse and reduce strong pro-inflammatory microgial activation in both hippocampal and cortical brain regions. If microglial inflammatory pathway inhibitors prove to be an effective method to control microglial activation, they can be used to correct chronically inflammaed microglia in AD environments. Such promise may lead to the exploration of a whole range of inhibitors that could prove as useful therapeutic strategies against AD.

WORKS CITED

Cherry, J. D. *et al.* (2014). Neuroinflammation and M2 microglia: the good, the bad, and the inflamed. *Journal of neuroinflammation 11*, 98.

Sarlus, H. and Heneka, M. T. (2017). Microglia in Alzheimer's disease. *The Journal of Clinical Investigation* 127(9):3240-3249.

Kaminska, B. *et al*. (2009). MPAK signal transduction underlying brain inflammation and gliosis as therapeutic target *The Anatomical Record*. 292(12).

Herlaar, E. and Brown, Z. (1999). p38 MAPK signaling cascades in inflammatory disease. *Molecular Medicine Today* 5(10):439-447.

Morrison, D. K. (2012). MAP Kinase Pathways. *Cold Spring Harb Persptives in Biology* 4(11).

Lisi, L. *et al.* (2016). Antiretrovirals inhibit arginase in human microglia. *Journal of Neurochemistry* 136:363-372.

Kankaanranta, H. *et al*. (1999). SB 203580, an inhibitor of p38 mitogen-activated protein kinase, enhances constitutive apoptosis of cytokine-deprived human eosinophils. *The Journal of Pharmacology and Experimental Therapeutics* 290(2):621-628.

Young, K. and Morrison, H. (2018). Quantifying microglia morphology from photomicrographs of immunohistochemistry prepared tissue using ImageJ. *Journal of Visualized Experiments* 136.

Arganda-Carreras, I. *et al.* (2010). 3D reconstruction of histological sections: application to mammary gland tissue. *Microscopy Research and Technique* 73(11):1019-1029.

R Core Team. (2020). R: A language and environment for statistical computing. R Foundation for Statistical Computing, Vienna, Austria. URL https://www.R-project.org/.

Stanko, J. P. *et al.* (2015). Application of sholl analysis to quantify changes in growth and evelopment in rat mammary gland whole mounts. *Reprod Toxicol* 54:129-135.

Fernandez-Arjona, M. M. *et al.* (2017). Microglia morphological categorization in a rat model of neuroinflammation by heirarchical cluster and principal components analysis. *Frontiers in Cellular Neuroscience* 11.

Heindi, S. *et al.* (2018). Automated morphological analysis of microglia after stroke. *Frontiers Cell Neuroscience* 12(106).